Journal of Integrative Neuroscience

J. Integr. Neurosci. **2026**; 25(9): 52923
https://doi.org/10.31083/JIN52923

Original Research

The Role of SPTLC2 and the MEK/ERK Signaling Pathway in the Metabolic Activity and Proliferation of Neural Stem Cells

Tianqing Liu[1,†], Bo Li[2,†], Folin Lan[1], Junlong Huang[1], Yuqin Ye[3], Xinhong Su[1,*]

[1]Department of Neurosurgery, Longyan First Affiliated Hospital of Fujian Medical University, 364000 Longyan, Fujian, China
[2]Department of Neurosurgery, The 960th Hospital of the PLA Joint Logistics Support Force, 250031 Jinan, Shandong, China
[3]Department of Neurosurgery, Xijing Hospital Affiliated to Air Force Medical University, 710032 Xi'an, Shaanxi, China
*Correspondence: xhsu415054@163.com (Xinhong Su)
[†]These authors contributed equally.

Academic Editor: Moo-Ho Won
Submitted: 14 April 2026 Revised: 2 July 2026 Accepted: 7 July 2026 Published: 21 September 2026

Abstract

Background: The use of neural stem cells (NSCs) to facilitate neurogenesis and improve impaired neural functions has attracted significant attention. Serine palmitoyltransferase long chain base subunit 2 (SPTLC2) induces apoptosis of neurons, while the mitogen-activated protein kinase (MEK)/extracellular signal-regulated kinase (ERK) pathway promotes NSC differentiation and proliferation. This study investigated the roles of SPTLC2 and the MEK/ERK pathway on the proliferation and metabolic activity of NSCs. **Methods:** SPTLC2 expression was altered through plasmid transfection and verified by Western blot and polymerase chain reaction (PCR) analyses. The effects of altered SPTLC2 expression on the metabolic activity and proliferation of NSCs were subsequently assessed using a cell counting kit and staining with 5-ethynyl-2'-deoxyuridine (EdU). Western blotting was used to examine the relationship between SPTLC2 and the MEK/ERK pathway by investigating changes in protein expression. To determine whether SPTLC2 acts via the MEK/ERK pathway, the activation state of this pathway was manipulated with U0126 and Erucin. Western blot and EdU staining were used to assess whether SPTLC2 affected the proliferation and metabolic activity of NSCs via the MEK/ERK pathway. **Results:** Plasmid transfection led to significant changes in SPTLC2 expression at both the mRNA ($p < 0.01$) and protein ($p < 0.05$) levels. SPTLC2 overexpression significantly reduced the proliferation and metabolic activity of NSCs ($p < 0.05$), whereas SPTLC2 knockdown mediated by siRNA significantly enhanced both parameters ($p < 0.05$). Western blot analysis revealed that the ratios of p-MEK/MEK and p-ERK/ERK were inversely correlated with the expression level of SPTLC2 ($p < 0.05$). Pharmacological modulation of the MEK/ERK pathway significantly reversed the SPTLC2-induced changes in pathway activity ($p < 0.05$) and partially restored the associated proliferative phenotypes. **Conclusions:** These findings indicate that SPTLC2 overexpression inhibits the proliferation and metabolic activity of NSCs, and that downregulation of SPTLC2 promotes these processes. The effects of SPTLC2 on NSCs were functionally associated with the MEK/ERK pathway.

Keywords: SPTLC2; MEK/ERK pathway; neural stem cells; metabolic activity; cell proliferation

1. Introduction

Neural stem cells (NSCs) have attracted significant attention in neuroscience and regenerative medicine because of their potential to differentiate into neurons, oligodendrocytes, and astrocytes. NSCs have self-renewal capacity and multiple-differentiation potential. Undifferentiated NSCs do not express mature cell antigens and are therefore less likely to be recognized and attacked by the immune system, making them safer for use in cell transplantation therapy [1]. NSCs were initially isolated primarily from neural tissue of the embryonic brain, such as the hippocampus and subventricular region [2]. Some specific areas of the adult brain, such as the dentate gyrus of the hippocampus and subependymal zone, also contain a small number of NSCs. These can be partially activated under certain conditions, such as injury, bleeding, ischemia, hypoxia, and alterations in the microenvironment [3,4]. Because of their differentiation potential, NSCs have been extensively studied as therapy for a variety of neurological conditions, such as multiple sclerosis, stroke, brain injury, Alzheimer's disease and Parkinson's disease [5,6,7]. NSCs can facilitate axon regeneration and myelination, accelerate the neuron repair process, and assist in improving the functional recovery of nerves [8]. Although NSCs have demonstrated great potential in the treatment of nervous system diseases, numerous challenges remain, including cell survival after transplantation, control of differentiation, immune response, and ethical issues. Future research is expected to address these challenges by optimizing the isolation, culture, and transplantation of NSCs, thereby facilitating their transition from basic research to clinical applications.

Serine palmitoyltransferase long chain base subunit 2 (SPTLC2) is a component of the serine palmitoyl transferase complex and plays a key role in sphingolipid biosynthesis [9]. Sphingolipids are important components of cell membranes and are indispensable for cell signaling. They maintain the structural integrity of cells and are involved in various cell signaling pathways. Sphingolipids are also

Copyright: © 2026 The Author(s). Published by IMR Press.
This is an open access article under the CC BY 4.0 license.

Publisher's Note: IMR Press stays neutral with regard to jurisdictional claims in published maps and institutional affiliations.

essential for maintaining the stability and function of cell membranes, as well as cell growth, differentiation, and apoptosis [10]. Through its key role in the synthesis of sphingolipids, SPTLC2 is therefore involved in cell membrane construction. One study showed that alterations in the activity of sphingolipid-metabolizing enzymes, such as ceramide synthase, influenced the survival and proliferation of NSCs [11]. The authors reported that inhibiting ceramide synthase increased the survival rate of NSCs and facilitated their proliferation. Another study reported that the direction of differentiation of NSCs into neurons or glial cells is influenced by the regulation of sphingolipid metabolism [12]. *SPTLC2* gene mutations have been associated with several genetic disorders, such as hereditary sensory autonomic neuropathy type 1C. This disorder affects the sensory and autonomic nervous systems, and patients may experience symptoms including sensory loss and autonomic dysfunction [13]. Enzymes that affect lipid metabolites, such as sphingosine kinase 2, can affect cell membrane properties, including the distribution and metabolic activity of receptors on the membrane. These changes can activate the mitogen-activated protein kinase (MEK)/extracellular signal-regulated kinase (ERK) pathway [14]. Sphingosine-1-phosphate (S1P) has been shown to affect the MEK/ERK signaling pathway [15], while SPTLC2 can influence the expression of S1P [16]. SPTLC2 can therefore directly or indirectly affect NSC differentiation and function by affecting lipid molecule formation. Considering the role of SPTLC2 in lipid metabolism and the extensive impact of the MEK/ERK pathway on cell function, SPTLC2 may indirectly affect cell metabolic activity and the MEK/ERK pathway by regulating the lipid environment of cell membranes. However, direct evidence is still lacking, and further verification of this hypothesis is required.

The MEK/ERK pathway has a crucial role in cell signaling and participates in a number of important biological processes, including cell proliferation, differentiation, growth, and apoptosis. MEK is a bispecific protein kinase that phosphorylates and activates downstream ERK protein kinases. ERK is a member of the mitogen-activated protein kinase family. Upon activation, it translocates to the nucleus and regulates the activity of transcription factors to influence gene expression. Under physiological conditions, the MEK/ERK pathway is critical for the regulation of cell growth, differentiation and survival, and for maintaining tissue homeostasis and development [17]. This pathway has been implicated in NSC proliferation, differentiation, migration, apoptosis and other processes [18,19,20]. In the current study, we investigated whether SPTLC2 influences the proliferation and metabolic activity of NSCs via the MEK/ERK pathway.

2. Materials and Methods

2.1 NSC Culture

Fourteen-day pregnant SD rats (Huafukang Bio, Beijing) were euthanized by CO_2 inhalation (30% chamber volume/min high-flow gradient ascent method). After confirmation of death, the animals were decapitated, and the fetuses were removed after alcohol disinfection. The cortical and hippocampal regions were isolated under sterile conditions and cut into small pieces in phosphate-buffered saline (PBS) on ice. After washing three times with D-Hank's solution, the tissues were incubated with a solution containing 0.125% trypsin and 0.02% ethylenediaminetetraacetic acid (EDTA, Solarbio, Beijing, China) for 10 min at 37 °C. The tissues were then dissociated using a 5 mL pipette and filtered through a copper mesh to eliminate tissue blocks from the cell suspension. The cell suspension was subsequently centrifuged (1000 ×g for 3 min), and the trypsin-EDTA solution was then removed. The cells were initially suspended in DMEM/F-12 (Keygenbio, Jiangsu, China) containing 10% fetal bovine serum (FBS) for post-digestion stabilization and washing. After washing three times (3x) with serum-free medium to completely remove FBS, the cells were resuspended in serum-free DMEM/F-12 containing 20 ng/mL each of basic fibroblast growth factor (bFGF) and epidermal growth factor (EGF) (Gibco, Grand Island, NY, USA) for long-term maintenance of NSCs. Half of this medium was changed every 2–3 days, and the cells were subcultured every 5–7 days. The NSCs were subcultured 3x and then seeded into 6-well plates at a density of 1×10^5 cells/mL for subsequent experiments. The plates had been previously coated with poly-L-ornithine (15 µg/mL, overnight at 37 °C) and laminin (10 µg/mL, 4 h at 37 °C).

2.2 Changes in SPTLC2 Expression After Transfection

Following the 2–3-day culture period, cells were transfected with the SPTLC2 overexpression vector and interference vector using Lipofectamine 2000 (Invitrogen, Carlsbad, CA, USA) as recommended by the manufacturer. pcDNA3.1-SPTLC2 (2 µg; ZHBY Bio, Nanchang, China) and Lipofectamine 2000 (10 µL) were diluted in 125 µL of Neurobasal medium (Gibco) and subsequently incubated at room temperature for 20 min. After washing 3x with PBS, the cells were incubated with transfection solutions for 6 h, after which the solutions were replaced with Neurobasal medium containing 0.5 mM glutamine (Gibco) and 2% B27 (Gibco). Similarly, small interfering (si)SPTLC2-356 (2 µg), siSPTLC2-739 (2 µg), siSPTLC2-1095 (2 µg), and empty vector as a negative control (NC) (2 µg) were individually transfected into cells using the same approach. The siRNA sequences targeting rat SPTLC2 are in **Supplementary Table 1**. The cells were assigned to groups as follows: control, SPTLC2 overexpression (OE) NC, SPTLC2 OE, si-SPTLC2 NC, and si-SPTLC2. The cells in each group were treated for 48 h for subsequent evaluation.

2.3 Identification of the Appropriate Concentrations of Erucin and U0126

Ten mg of Erucin (#HY-121323, MedChemExpress LLC, Shanghai, China) was dissolved in 1.55 mL dimethyl sulfoxide (DMSO) to give a 40 mM stock solution, and 10 mg of U0126 (#HY-12031, MedChemExpress) was dissolved in 1.172 mL of DMSO to prepare a 20 mM stock solution. These stock solutions were then diluted to achieve drug concentrations of 0, 1, 2, 5, 10, and 20 µM. The experimental procedures for determining cell metabolic activity using the CCK-8 assay are described in Section 2.7.

2.4 Quantitative Real-Time Polymerase Chain Reaction (qPCR)

Total RNA was extracted from cells using TRIzol reagent (Wanleibio, Shenyang, China), with mRNA subsequently isolated using an RNA ultrapure extraction kit (Wanleibio). The mRNA concentration and purity (OD260/OD280) were determined with an ultraviolet–visible spectrophotometer (UV2500, Tianmei Instrument, Shanghai, China). An RNA reverse transcription kit (Sangon Biotech, Shanghai, China) was used to synthesize cDNA. Fluorescence quantitative PCR (Bole Life Medical Products Co., Ltd., Shanghai, China) was performed under the following cycling conditions: pre-denaturation for 10 min at 95 °C, then 40 cycles of denaturation for 10 s at 95 °C, annealing for 30 s at 58 °C, and extension for 30 s at 72 °C. The $2^{\wedge-\Delta\Delta Ct}$ method was used to calculate relative gene expression, with Glyceraldehyde 3-phosphate dehydrogenase (*GAPDH*) used as the internal reference. Table 1 lists the primer sequences.

Table 1. Primer sequences for SPTLC2 and GAPDH.

Primer	Sequence (5′-3′)
GAPDH_F	GACAACTTTGGCATCGTGGA
GAPDH_R	ATGCAGGGATGATGTTCTGG
SPTLC2_F	ACTGTCGGGAGCAACCATTC
SPTLC2_R	CGAACAATAGACCCTTCCATGCT

SPTLC2, serine palmitoyltransferase long chain base subunit 2; GAPDH, Glyceraldehyde 3-phosphate dehydrogenase.

2.5 Western Blotting

Cells were first washed with PBS, incubated in lysis buffer (Sangon), then scraped to one side and drawn into a labeled Eppendorf (EP) tube using a pipette. They subsequently underwent complete disruption using a cell disruptor. Following centrifugation (12,000 r/min for 10 min), the supernatant was removed and placed into a new EP tube. Bicinchoninic acid (BCA) buffer solution (Sangon) was then added, and the EP tube was placed into boiling water for 5 min before measuring the protein concentration using the BCA method. The volume of sample for loading onto the gel was then adjusted to give 6 µg of protein in each well. Proteins underwent separation using sodium dodecyl sulfate–polyacrylamide gel electrophoresis (SDS–PAGE; Wanleibio) and were subsequently transferred onto a polyvinylidene fluoride membrane (Millipore, Billerica, USA). A 5% skim milk powder solution was used to block the membrane before incubating overnight at 4 °C with primary antibodies against the following proteins: SPTLC2 (1:1000, #51012-2-AP, Proteintech, Chicago, IL, USA), MEK1/2 (1:1000, #af6385, Affinity Biosciences, Cincinnati, OH, USA), p-MEK1/2 (1:1000, #DF7768, Affinity), ERK1/2 (1:1000, #AF0155, Affinity), p-ERK1/2 (1:1000, #AF1015, Affinity), and β-Actin (1:2000, #HC201, TransGenbiotech, Beijing, China). The horseradish peroxidase (HRP)-conjugated secondary antibodies were goat anti-mouse IgG (H+L) (1:2000; #GB23301; Servicebio, Wuhan, China) or goat anti-rabbit IgG (H+L) (1:2000; #GB23303; Servicebio). Enhanced chemiluminescence solution (Wanleibio) was subsequently used to visualize the protein bands.

2.6 Immunofluorescence Staining

Cells were fixed in 4% paraformaldehyde for 15 min, washed 3x in PBS, permeabilized with 0.5% Triton X-100 for 15 min, washed again 3x with PBS, and subsequently incubated for 30 min with blocking buffer (Beyotime, Beijing, China). They were then incubated at 4 °C overnight with anti-nestin antibody (1:200; #DF7754; Affinity Biosciences). After washing, a fluorescent secondary antibody (1:200; #AS007; ABclonal Technology, Wuhan, China) was added. Finally, the nuclei were stained with 4',6-diamidino-2-phenylindole (DAPI, #KGE2505-10; KeyGen Bio, Nanjing, China) and the samples examined under a fluorescence microscope (CKX53; Olympus, Tokyo, Japan). Nestin-positive cells were recorded at 400× magnification. Cells with clear nuclear DAPI staining and cytoplasmic/membranous nestin fluorescence above the background threshold were counted as positive. The percentage was calculated as follows: (nestin-positive cells / total DAPI-positive cells) × 100%.

2.7 CCK-8 Assay

In accordance with Section 2.2, 96-well plates were prepared and labeled for grouping after cell transfection. To each well, 100 µL of cell suspension was added, and the cells were cultured for 24 h at 37 °C in a 5% CO_2 incubator. Subsequently, CCK-8 reagent (KeyGen Bio) was added (10 µL), and incubation continued for a further 2 h. Finally, the absorbance at 450 nm wavelength was measured in each well using an enzyme labeling instrument (WD-2012B, Beijing 61 Instrument Factory, Beijing, China). Various concentrations of Erucin or U0126 were prepared as described in Section 2.3. Following treatment with these compounds, the cell metabolic activity of NSCs was evaluated using the previously described CCK-8 assay.

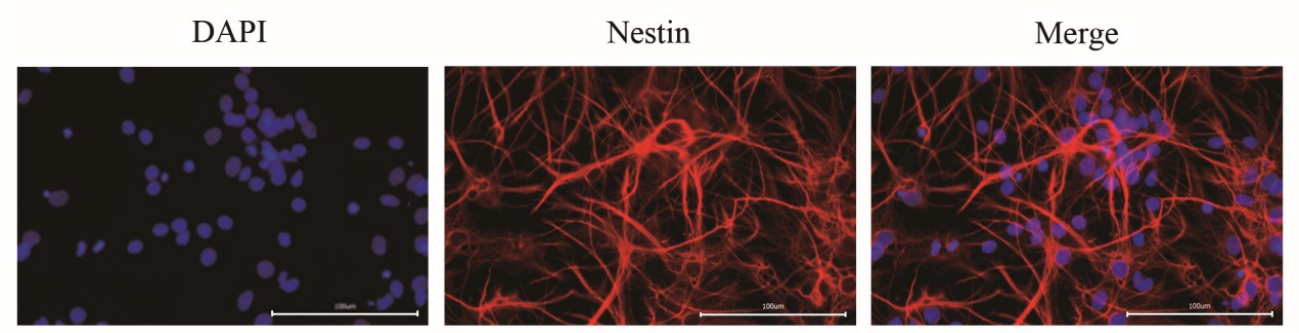


Fig. 1. Identification of neural stem cells (NSCs) using fluorescence staining. NSCs were immunostained using antibodies against nestin. Scale bar: 100 µm (400× magnification). DAPI, 4',6-diamidino-2-phenylindole.

2.8 EdU Cell Proliferation Assay

Cell proliferation capacity was assessed with the 5-ethynyl-2'-deoxyuridine (EdU) assay kit (Beyotime). Cells were assigned to the following groups: control, control + DMSO, control + NC, SPTLC2 OE, SPTLC2 OE + NC, si-SPTLC2, si-SPTLC2 + NC, SPTLC2 OE + si-SPTLC2, SPTLC2 OE + Erucin, and si-SPTLC2 + U0126. Following the above treatment for 48 h, cells were incubated with EdU working solution (10 µM) diluted in fresh medium for 2 h. After removal of the supernatant, the cells were fixed for 15 min with 4% paraformaldehyde and then incubated with 0.5% Triton X-100 for 10 min at room temperature. Click reaction solution was subsequently added to the samples and incubated for 30 min in the dark. After each step, the cells were rinsed with PBS 3x for 3 min each. Cell nuclei were then counterstained with 1 mL of 1x Hoechst 33342 (Beyotime) and kept in the dark for 10 min at room temperature. After removing Hoechst 33342 solution, the cells were subsequently washed 3x with PBS for 3 min each before observation under a fluorescence microscope (Olympus). EdU-positive cells were identified by red fluorescence signal exceeding the threshold set by the negative control samples. The total cell number was determined by DAPI-stained nuclei, and the EdU labeling index was calculated as follows: (EdU-positive cells / total DAPI-positive cells) × 100%.

2.9 Statistical Analysis

GraphPad Prism (V8, GraphPad Software Inc., San Diego, CA, USA) and ImageJ (V1.8.0, NIH, Bethesda, MD, USA) were used to analyze the data, with experiments repeated at least three times. The data represent the average of three independent experiments and are presented as the mean ± standard deviation (SD). For experiments in which all treatment conditions were processed in parallel within each independent experiment (i.e., cells from the same batch and passage were split and treated simultaneously), repeated-measures one-way ANOVA was used for the overall comparison among groups, followed by paired two-tailed *t*-tests for pre-specified pairwise comparisons. For comparisons between two independent groups, an unpaired two-tailed *t*-test was used, and one-way ANOVA followed by Tukey's multiple comparisons test was applied for multiple independent groups. A p-value of < 0.05 was used as the threshold for statistical significance.

3. Results

3.1 Immunofluorescence Identification of NSCs

First, the cultured cells were confirmed to be NSCs. As shown in Fig. 1, bright red fluorescence was observed under a fluorescence microscope, indicating positive expression of nestin, a marker of NSCs. This result confirmed the cultured cells were NSCs and thus suitable for further studies.

3.2 Verification of the Transfection Efficiency of SPTLC2 Overexpression and Interference Vectors Using qPCR and Western Blot

We investigated the effect of transfection on SPTLC2 expression, and also identified and validated the most appropriate intervention conditions. The results of qPCR and Western blot indicated significantly more SPTLC2 expression in the overexpression (OE) group than in the OE negative control (NC) group. Conversely, SPTLC2 was lower in the Si-SPTLC2-1095 group compared to the interference NC group. In subsequent experiments, the Si-SPTLC2-1095 group is designated the Si-SPTLC2 group (Fig. 2).

3.3 CCK-8 Assay to Assess the Effect of SPTLC2 Expression on NSC Metabolic Activity

The metabolic activity of NSCs was evaluated using the CCK-8 assay. The cell metabolic activity of the SPTLC2-OE group was lower than that of the control and SPTLC2-OE-NC groups. Conversely, cell metabolic activity was higher in the si-SPTLC2 group compared to the control group and si-SPTLC2-NC group (Fig. 3). The above findings suggest that overexpression of SPTLC2 inhibits the metabolic activity of NSCs, whereas decreased expression of SPTLC2 enhances the metabolic activity of NSCs.

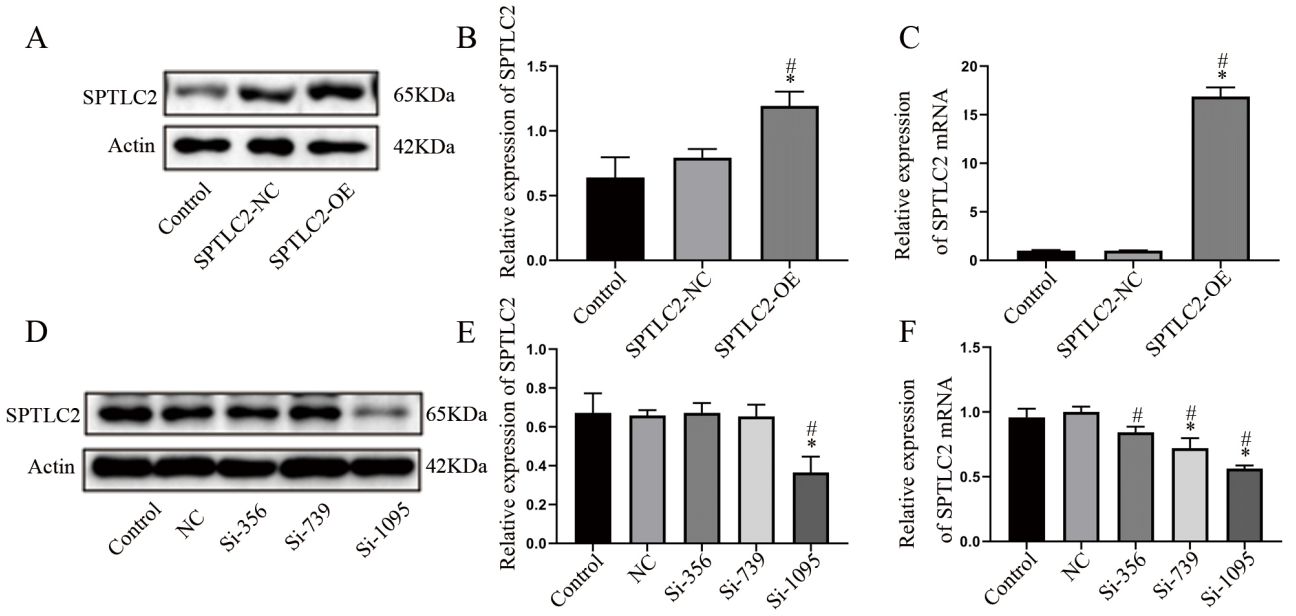


Fig. 2. Verification of the transfection efficiency of SPTLC2 overexpression and interference vectors. (A,D) Western blotting to assess SPTLC2 expression. (B,E) Quantification of Western blots. (C,F) *SPTLC2* expression was quantified using quantitative real-time polymerase chain reaction (qPCR), with *GAPDH* serving as the control. The results shown represent the mean ± standard deviation (SD) of three experiments. $^{*}p < 0.05$ vs. control group. $^{\#}p < 0.05$ vs. negative control (NC) group. OE, overexpression.

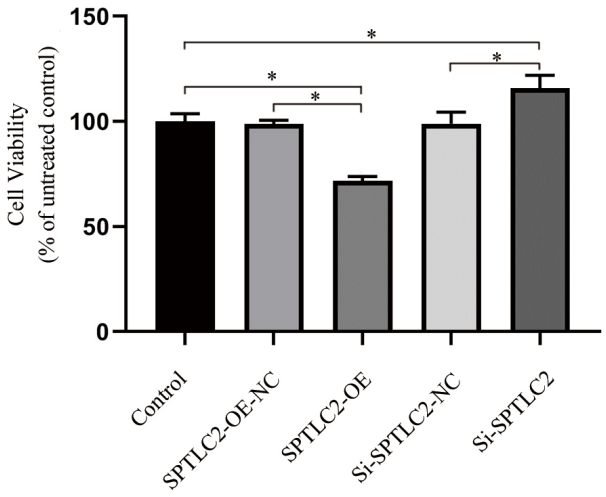


Fig. 3. Effect of SPTLC2 expression on the metabolic activity of NSCs. The data shown represent the mean ± SD from three experiments. $^{*}p < 0.05$.

3.4 SPTLC2 Expression and the Proliferation of NSCs

In this experiment, we used the EdU assay to examine the impact of SPTLC2 expression on NSC proliferation. Nuclei stained with DAPI display blue fluorescence, while proliferating cells with EdU staining exhibit red fluorescence (Fig. 4). A lower level of red fluorescence was found in the SPTLC2-OE group compared to the control and SPTLC2-OE-NC groups, indicating reduced cell proliferation. Conversely, the higher level of red fluorescence in the Si-SPTLC2 group compared with the si-SPTLC2-NC group indicates enhanced cell proliferation (Fig. 4). This finding suggests that overexpression of SPTLC2 inhibits NSC proliferation, whereas decreased expression of SPTLC2 enhances the proliferation of NSCs.

3.5 SPTLC2 Expression and the MEK/ERK Pathway

Next, Western blot analysis was performed to determine whether SPTLC2 expression affects protein expression within the MEK/ERK signaling pathway. The SPTLC2 protein ratio was significantly higher in the SPTLC2-OE group compared to the SPTLC2-OE-NC group, whereas p-MEK/MEK and p-ERK/ERK ratios were significantly lower. In contrast, the si-SPTLC2 group had significantly lower expression of SPTLC2 protein than the si-SPTLC2-NC group, while the p-MEK/MEK and p-ERK/ERK ratios were significantly higher in the si-SPTLC2 group (Fig. 5). These findings suggest that SPTLC2 expression is inversely proportional to the activation state of the MEK/ERK pathway.

3.6 Selection of Appropriate Concentrations of Erucin and U0126

Erucin is an isothiocyanate that is abundant in arugula. It exerts anticancer, neuroprotective and anti-inflammatory effects and is also an efficient activator of the MEK/ERK pathway [21,22,23]. In contrast, U0126 is an inhibitor of the MEK/ERK pathway. It inhibits MEK1 and MEK2 activities in a noncompetitive manner, thereby preventing them from phosphorylating ERK1/2 [24,25]. We prepared

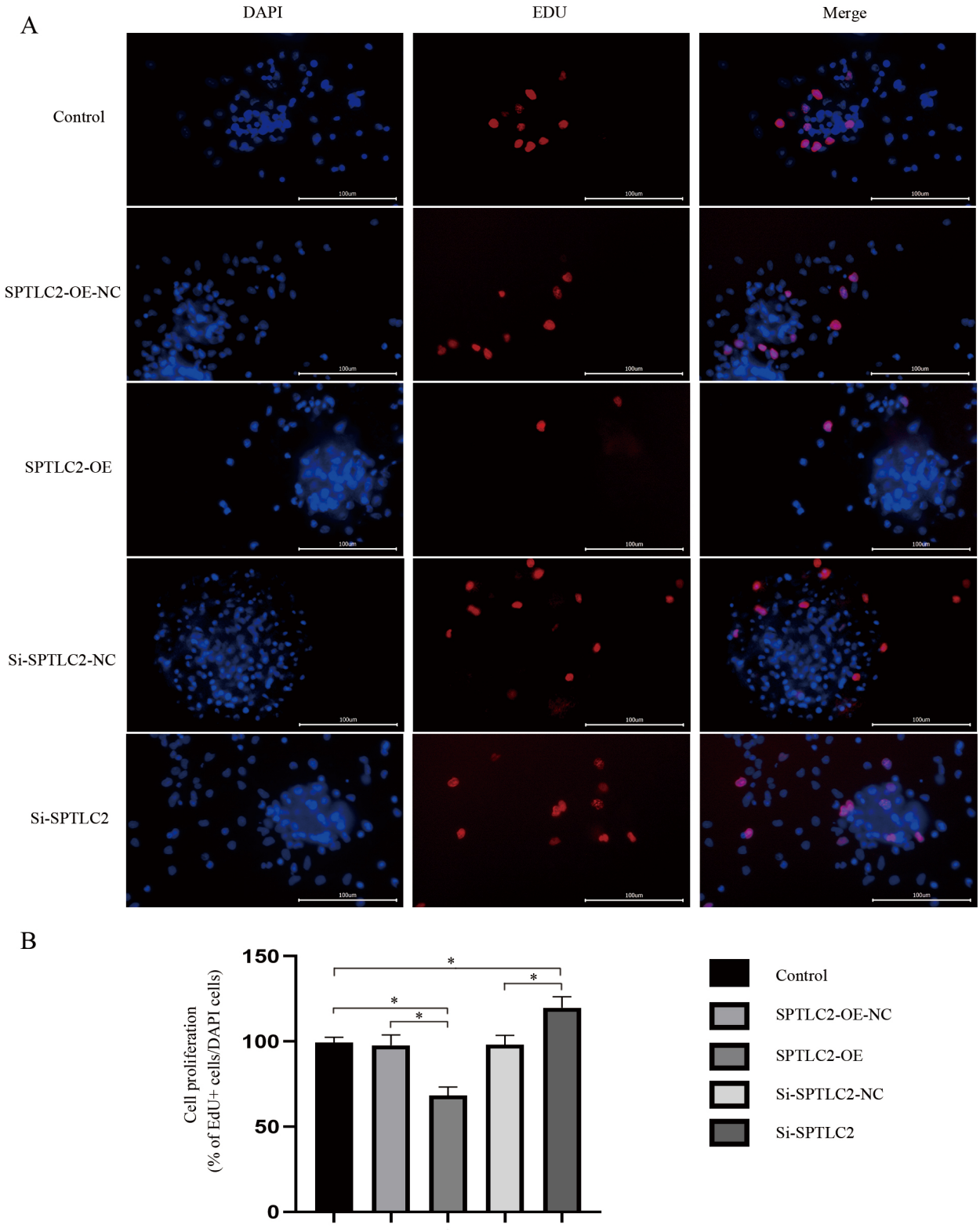


Fig. 4. SPTLC2 expression and the proliferation of NSCs. (A) EdU fluorescence staining (400× magnification). (B) Quantification of 5-ethynyl-2'-deoxyuridine (EdU) fluorescence staining. The results shown represent the mean ± SD of three experiments. $^{*}p < 0.05$. Scale bar: 100 μm.

Erucin and U0126 at concentrations of 0, 1, 2, 5, 10 and 20 μM and examined their effects on cell metabolic activity using the CCK-8 assay to determine the optimal concentrations. At a concentration of 10 μM, Erucin significantly

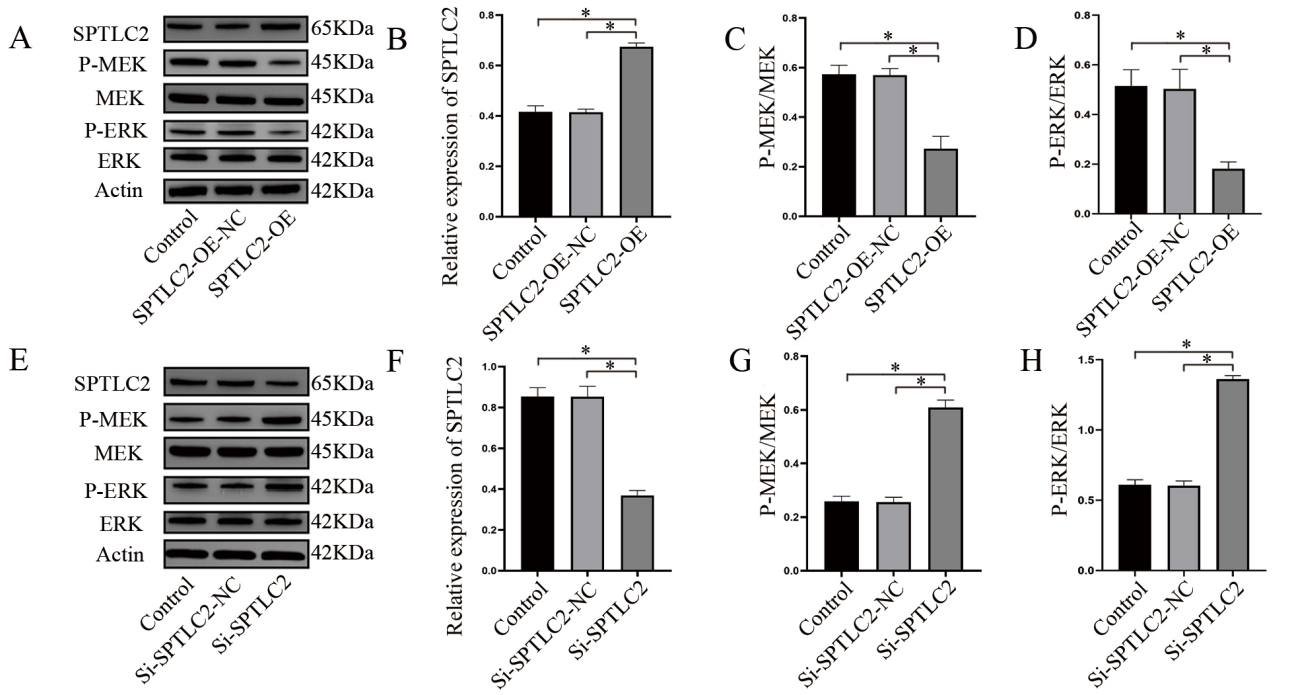


Fig. 5. SPTLC2 expression correlates inversely with the expression of proteins linked to the mitogen-activated protein kinase (MEK)/extracellular signal-regulated kinase (ERK) pathway. (A,E) Western blot detection of SPTLC2, p-MEK, MEK, p-ERK, and ERK proteins. (B–D,F–H) Quantification of Western blot data, with actin serving as a control. The results shown are the mean ± SD from three experiments. $^{*}p < 0.05$.

promoted cell metabolic activity, whereas at 20 µM it inhibited cell metabolic activity (Fig. 6A). U0126 significantly inhibited cell metabolic activity at concentrations of 5, 10 and 20 µM (Fig. 6B). Therefore, in subsequent experiments we used Erucin at a concentration of 10 µM and U0126 at a concentration of 5 µM.

3.7 SPTLC2 Expression and NSC Proliferation

This experiment was conducted to examine the effect of SPTLC2 on NSCs and to exclude the possible influence of the solvent DMSO. Cells treated with DMSO exhibited no significant change in cell proliferation. The difference in SPTLC2 protein expression between the control and control + DMSO groups did not reach statistical significance. After transfection with the SPTLC2 OE vector, the protein expression of SPTLC2 increased significantly, while the proliferative capacity of NSCs decreased significantly. Conversely, when cells transfected with the SPTLC2 OE vector were subsequently transfected with the SPTLC2 interference vector, SPTLC2 protein expression decreased, and the proliferation ability of NSCs increased significantly (Fig. 7).

3.8 Erucin Increases and U0126 Suppresses the Expression of MEK/ERK Pathway Proteins

We next examined whether an activator or inhibitor of the MEK/ERK pathway could reverse the impact that SPTLC2 has on this pathway. Our goal was to determine whether the effect of SPTLC2 on the proliferation of NSCs occurs via the MEK/ERK pathway. Following overexpression of SPTLC2 in the SPTLC2-OE group, the ratios of pMEK/MEK and pERK/ERK decreased significantly. SPTLC2 protein expression was lower in the SPTLC2-OE + Erucin group than in the SPTLC2-OE group, and the pMEK/MEK and pERK/ERK ratios were significantly higher. Following suppression of SPTLC2 protein expression, the ratios of pMEK/MEK and pERK/ERK increased significantly. Higher protein expression of SPTLC2 was observed in the si-SPTLC2 + U0126 group compared to the si-SPTLC2 group, while the ratios of pMEK/MEK and pERK/ERK were significantly decreased (Fig. 8). These results indicate that Erucin and U0126 can partially alter the impact that SPTLC2 has on the MEK/ERK pathway.

3.9 SPTLC2 Effects on NSC Proliferation Are Functionally Coupled With the MEK/ERK Pathway

We next assessed NSC proliferation after manipulating MEK/ERK pathway activity. NSC proliferative capacity decreased significantly after transfection with the SPTLC2 OE vector, which was partially restored by treatment with Erucin (although this trend did not reach statistical significance). Transfection with the si-SPTLC2 vector significantly increased the proliferative capacity of NSCs, which was attenuated by treatment with U0126 (although this trend did not reach statistical significance) (Fig. 9).

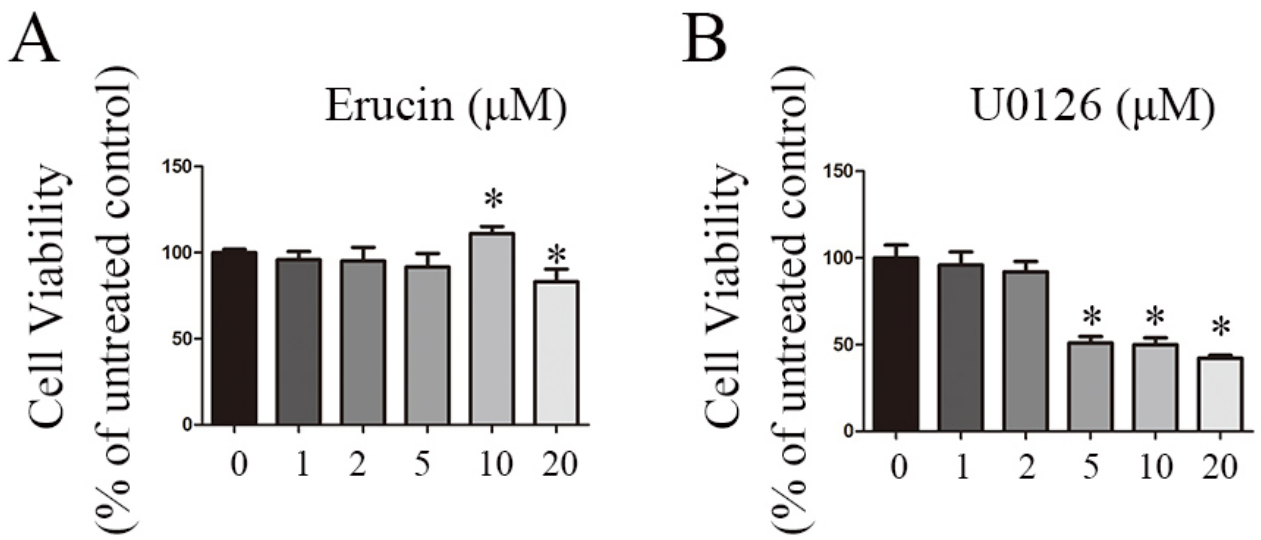


Fig. 6. Identification of the optimal concentrations of Erucin and U0126 for subsequent experiments. (A) Erucin drug concentration test. (B) U0126 drug concentration test. The data shown are the mean ± SD from three experiments. $^{*}p < 0.05$ vs. 0 μM group.

Collectively, the above results suggest that SPTLC2 may regulate NSC proliferation via the MEK/ERK pathway.

4. Discussion

The modulation of SPTLC2 expression or MEK/ERK pathway activation status revealed that SPTLC2 significantly affects the proliferation and metabolic activity of NSCs. Moreover, this effect is functionally coupled with the MEK/ERK pathway. This study provides *in vitro* evidence that SPTLC2 inhibits NSC proliferation and metabolic activity, while also investigating the possible mechanism. Using the CCK-8 assay and EdU staining, the proliferation and metabolic activity of NSCs were found to decrease when SPTLC2 was overexpressed, but increase when SPTLC2 was downregulated. In addition, SPTLC2 expression levels were inversely correlated with the MEK/ERK pathway activation status. Therefore, we infer that SPTLC2 influences NSCs via the MEK/ERK pathway, although the present data demonstrate functional coupling rather than a molecular mechanism.

The MEK/ERK pathway has a critical role in regulating the proliferation of NSCs. Several growth factors (e.g., EGF, FGF) and cytokines promote NSC proliferation via MEK/ERK pathway activation [26]. ERK activation regulates the expression of cell cycle genes, thereby propelling cells into the division cycle. The MEK/ERK pathway also has an important role in maintaining the survival of NSCs [27]. ERK activation inhibits apoptotic pathways and promotes the expression of anti-apoptotic proteins, thereby protecting NSCs from various stress factors. We observed a clear inverse relation between the metabolic activity/proliferation of NSCs and SPTLC2 expression. To determine whether SPTLC2 regulates NSC metabolic activity and proliferation via the MEK/ERK pathway, we manipulated SPTLC2 expression and applied pharmacological activators and inhibitors of the MEK/ERK pathway. After transfection with the SPTLC2 OE vector, cell metabolic activity and proliferation decreased significantly, while cell metabolic activity and proliferation improved after subsequent treatment with Erucin. Conversely, after transfection with si-SPTLC2, cell metabolic activity and proliferation increased significantly, whereas subsequent treatment with U0126 reduced both parameters. These results demonstrate the following functional interaction: MEK/ERK pathway activation alleviates the inhibitory effect of high SPTLC2 expression on NSC metabolic activity and proliferation, whereas inhibition of this pathway exacerbated these effects. Based on the literature, we speculate that SPTLC2 can influence the MEK/ERK pathway through multiple mechanisms. First, SPTLC2 may catalyze the generation of S1P, which can bind to sphingosine-1-phosphate receptor1/3 and potentially activate the MEK/ERK pathway [28]. Second, intracellular S1P, as a second messenger, may directly bind to and inhibit histone deacetylase1/2, resulting in histone acetylation. This could lead to overexpression of dual-specificity phosphatase 6 and the dephosphorylation of ERK, potentially forming a negative feedback loop [29,30,31]. The latter mechanism could explain why MEK/ERK activity declined when SPTLC2 was overexpressed. However, this interpretation conflicts with the first hypothesis, possibly because of the localization and mechanism of action of S1P, and therefore requires further research. Third, excessive SPTLC2 expression may drive ceramide accumulation, which could activate protein phosphatase 2A, potentially leading to the dephosphorylation of rapidly accelerated fibrosarcoma (RAF) proteins, thereby

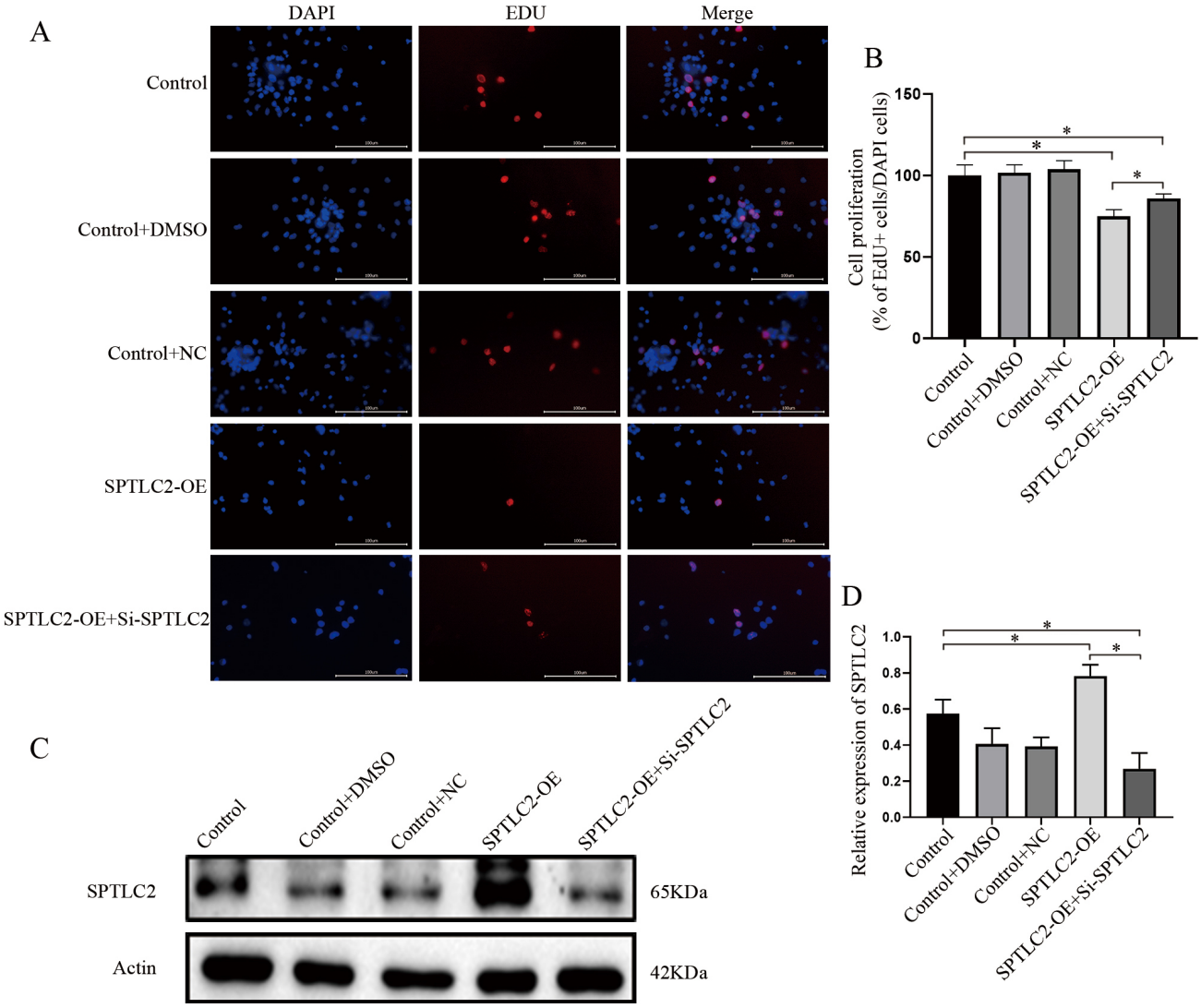


Fig. 7. SPTLC2 inhibits NSC proliferation. (A) The proliferative capacity of NSCs was analyzed using EdU staining (400× magnification). (B) Quantification of EdU fluorescence staining. (C) Western blot detection of SPTLC2 expression. (D) Quantification of Western blots, with actin serving as a control. Results shown are the mean ± SD from three experiments. $^{*}p < 0.05$. Differences between Control, Control + DMSO, and Control + NC groups did not reach statistical significance ($p > 0.05$). Scale bar: 100 μm. DMSO, dimethyl sulfoxide.

inhibiting the MEK/ERK pathway [32,33]. Fourth, by altering the sphingolipid-to-cholesterol ratio, SPTLC2 may disrupt lipid-raft integrity, potentially modulating EGF receptor clustering and affecting MEK/ERK pathway activity [34,35]. Finally, SPTLC2 may alter the composition of mitochondrial sphingolipids, thereby affecting electron transport chain efficiency and altering production of reactive oxygen species. This could activate redox-sensitive phosphatases, potentially leading to dephosphorylation of ERK [36].

Several limitations of this study should be acknowledged. Conventional *in vitro* models lack the intricate cellular crosstalk among neurons, vascular compartments and immune cells, and therefore cannot fully simulate the complex brain microenvironment. As yet, there is no evidence to support a direct interaction between SPTLC2 and components of the MEK/ERK pathway. A comprehensive literature search and interrogation of protein interaction databases (e.g., STRING, BioGRID) failed to reveal any documented physical association between SPTLC2 and MEK/ERK pathway constituents. Future studies should therefore employ co-immunoprecipitation or fluorescence co-localization assays to identify potential direct binding partners of SPTLC2. Our experimental results do not exclude the possibility that cell cycle arrest serves as a confounding factor. The CCK-8 assay measured cellular metabolic activity rather than cell viability. Future studies using time-course analysis of cell cycle distribution

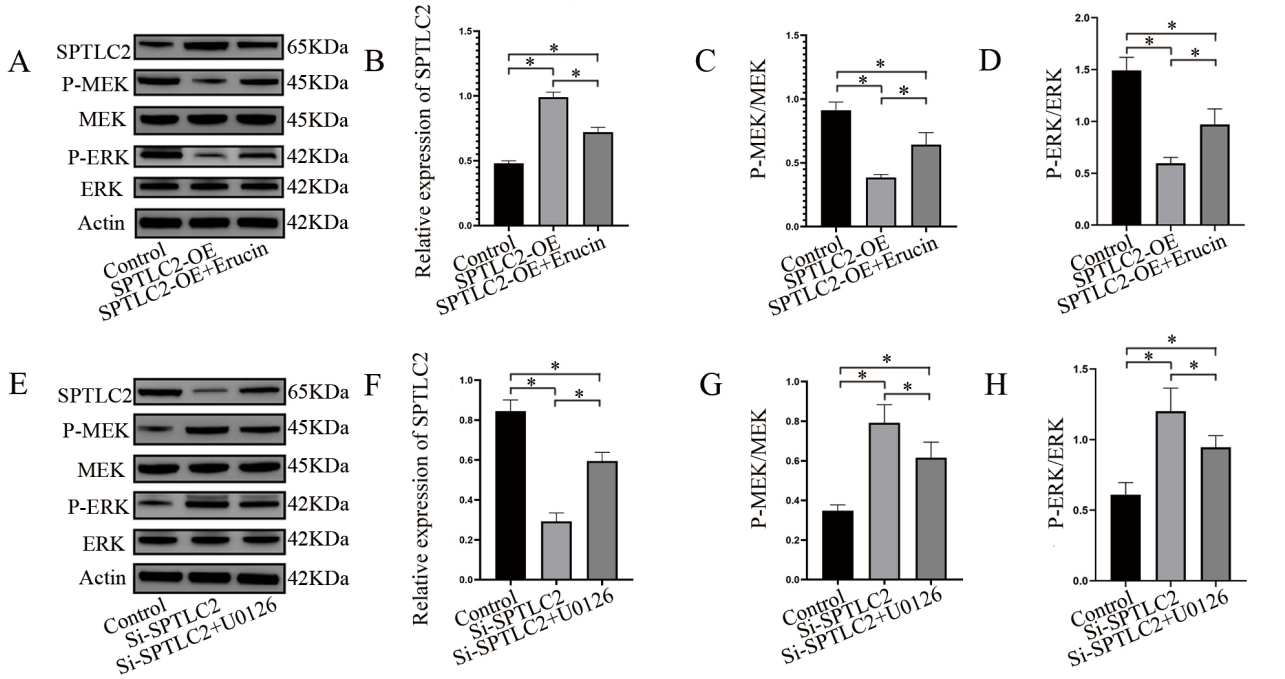


Fig. 8. The effects of Erucin and U0126 on SPTLC2 and the MEK/ERK pathway. (A,E) Western blot analysis of SPTLC2, p-MEK, MEK, p-ERK, and ERK proteins. (B–D,F–H) Quantification of Western blot data, with actin serving as the control. The results shown are the mean ± SD of three experiments. $^{*}p < 0.05$.

and DNA synthesis rates (EdU/BrdU incorporation), Annexin V/PI apoptosis assays, and Ki67 immunostaining are needed to definitively establish the underlying mechanism. We also acknowledge that relying solely on EdU incorporation to assess cell proliferation dynamics has limitations. EdU labels S-phase cells but does not provide information on the rate of cell cycle progression, G1/S transition efficiency, or the proportion of quiescent (G0) cells. The inclusion of cell-cycle markers such as Cyclin D1, p21, or Ki67 in future studies should provide a more comprehensive picture of proliferation kinetics. It is important to emphasize that the pharmacological interventions with Erucin and U0126 do not establish direct pathway specificity for the observed functional association between SPTLC2 and NSC proliferation. Erucin exerts pleiotropic biological effects beyond MEK/ERK activation, including antioxidant activity and Nrf2 pathway activation [21,23]. Therefore, the rescue effect observed with Erucin treatment could not be exclusively attributed to reactivation of the MEK/ERK pathway. An additional critical caveat in interpreting our pharmacological rescue data is that both Erucin and U0126 treatments per se altered endogenous SPTLC2 protein levels (Fig. 8). Consequently, the pharmacological rescue experiments cannot unambiguously determine whether the observed phenotypic effects are mediated by the MEK/ERK pathway or by drug-induced modulation of SPTLC2 expression, or both. Future studies employing genetic approaches to specifically modulate MEK/ERK activity without concomitant changes in SPTLC2 levels (e.g., CRISPR-mediated MEK1/2 knockout in SPTLC2-overexpressing cells) will be necessary to resolve this ambiguity and establish a clearer causal relationship. However, we found that Erucin/U0126 treatment reversed the molecular signature and largely restored the functional phenotype of SPTLC2-manipulated NSCs toward baseline. Collectively, our results provide convergent evidence to support involvement of the MEK/ERK pathway in this process.

Given its critical role in NSCs, targeted modulation of MEK/ERK is being explored as a therapeutic strategy for neurological disorders. For instance, activation of this pathway facilitates NSC proliferation and differentiation, thereby promoting the repair and regeneration of nerve damage. Since the MEK/ERK pathway plays a critical role in the biological function of NSCs, a deeper understanding of its mechanisms may yield novel therapeutic strategies and molecular targets for neurological diseases. However, NSC-based therapies carry the risk of tumorigenesis [37]. The MEK/ERK pathway is associated with tumor formation, and it remains to be determined whether modulation of this pathway via SPTLC2 can suppress tumor formation during NSC therapy. In theory and under certain conditions, NSCs are highly operable, with the ability to bypass the blood–brain barrier and contribute to the repair of damaged neural functions [38,39,40]. Nevertheless, NSC therapy currently encounters difficulties in maintaining cell metabolic activity and function during implantation *in vivo* [41]. This may lead to a low survival rate and poor prognosis for transplanted NSCs. If verified *in vivo*, mod-

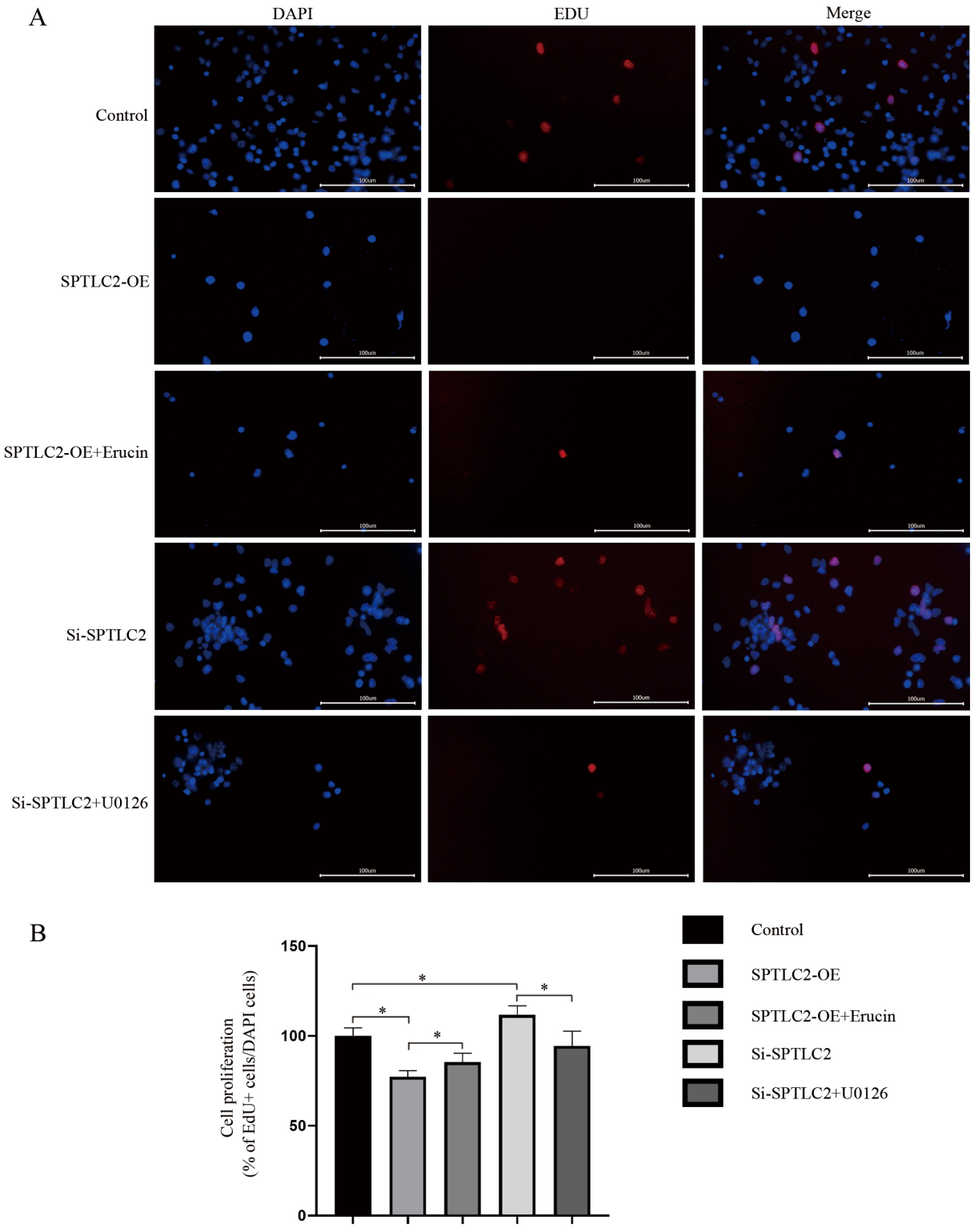


Fig. 9. Effects of different treatments on the proliferative capacity of NSCs. (A) EdU fluorescence staining (400× magnification). (B) Quantification of EdU fluorescence staining. The results shown are the mean ± SD from three experiments. $^{*}p < 0.05$. $^{NS}p > 0.05$. Scale bar: 100 μm.

ulating the activity of SPTLC2 may open new possibilities for NSCs in the transplantation environment by enhancing their survival and proliferation, thus offering a novel approach for clinical treatment.

5. Conclusion

Our results showed that SPTLC2 overexpression inhibits the proliferation and metabolic activity of NSCs via the MEK/ERK pathway, whereas downregulation of SPTLC2 enhances these processes through the same pathway. Moreover, SPTLC2 represents a potential drug target, and modulating its activity may provide novel therapeutic strategies for diseases characterized by aberrant sphingolipid metabolism. Further investigation of SPTLC2 should further clarify the underlying disease mechanisms and facilitate the development of new treatments.

Availability of Data and Materials

The datasets are available in the Zenodo repository (https://doi.org/10.5281/zenodo.22710566).

Author Contributions

TL: Conceptualization; Data curation; Experimental implementation; project administration; Writing-original draft; review and editing; Visualization; Interpretation of results. BL: Manuscript editing and revision; Data analysis and validation; Figure revision. FL: Experimental implementation. JH: Data analysis; Proofreading. YY: Formal analysis, Funding acquisition. XS: Data curation, Experimental implementation, Writing-original draft, Funding acquisition. All authors contributed to editorial changes in the manuscript. All authors read and approved the final manuscript. All authors have participated sufficiently in the work and agreed to be accountable for all aspects of the work.

Ethics Approval and Consent to Participate

The pregnant SD rats at 14 days were purchased from Beijing HuaFuKang Biotechnology Co., Ltd. (License No. SCXK (Beijing) 2019-0008). All animal procedures were performed by Jiangxi Zhonghong Boyuan Biotechnology Co., Ltd., which was licensed by the Experimental Animal Ethics Committee of Jiangxi Zhonghong Boyuan Biotechnology Co., Ltd. (Approval Number: LL202303240003). Subsequent in vitro cell culture and experimental assays were conducted at Longyan First Affiliated Hospital of Fujian Medical University. All animal experiments were conducted in accordance with relevant guidelines (the ARRIVE 2.0 guideline) and regulations (Guidelines for the Management and Use of Laboratory Animals).

Acknowledgment

We thank Jiangxi Zhonghong Boyuan Biotechnology Co., Ltd. (Nanchang, China) for the isolation and culture of neural stem cells.

Funding

This study was sponsored by Longyan City Science and Technology Plan Project (2022LYF17098), Natural Science Foundation of Hunan Province (2023JJ30432), and Excellent Youth Science Research Project of Hunan Education Department (22B0095).

Conflicts of Interest

The authors declare no conflicts of interest. The funding bodies and relevant experimental institution did not interfere with or influence the conduct of the experiments.

Supplementary Material

Supplementary material associated with this article can be found, in the online version, at https://doi.org/10.31083/JIN52923.

References

[1] Vieira MS, Santos AK, Vasconcellos R, Goulart VAM, Parreira RC, Kihara AH, et al. Neural stem cell differentiation into mature neurons: Mechanisms of regulation and biotechnological applications. Biotechnology Advances. 2018; 36: 1946–1970. https://doi.org/10.1016/j.biotechadv.2018.08.002

[2] Matarredona ER, Zarco N, Castro C, Guerrero-Cazares H. Editorial: Neural Stem Cells of the Subventricular Zone: From Neurogenesis to Glioblastoma Origin. Frontiers in Oncology. 2021; 11: 750116. https://doi.org/10.3389/fonc.2021.750116

[3] Gonçalves JT, Schafer ST, Gage FH. Adult Neurogenesis in the Hippocampus: From Stem Cells to Behavior. Cell. 2016; 167: 897–914. https://doi.org/10.1016/j.cell.2016.10.021

[4] Llorente V, Velarde P, Desco M, Gómez-Gaviro MV. Current Understanding of the Neural Stem Cell Niches. Cells. 2022; 11: 3002. https://doi.org/10.3390/cells11193002

[5] Chen C, Chang ZH, Yao B, Liu XY, Zhang XW, Liang J, et al. 3D printing of interferon γ-preconditioned NSC-derived exosomes/collagen/chitosan biological scaffolds for neurological recovery after TBI. Bioactive Materials. 2024; 39: 375–391. https://doi.org/10.1016/j.bioactmat.2024.05.026

[6] Culig L, Chu X, Bohr VA. Neurogenesis in aging and age-related neurodegenerative diseases. Ageing Research Reviews. 2022; 78: 101636. https://doi.org/10.1016/j.arr.2022.101636

[7] Peruzzotti-Jametti L, Bernstock JD, Willis CM, Manferrari G, Rogall R, Fernandez-Vizarra E, et al. Neural stem cells traffic functional mitochondria via extracellular vesicles. PLoS Biology. 2021; 19: e3001166. https://doi.org/10.1371/journal.pbio.3001166

[8] Nekanti U, Sakthivel PS, Zahedi A, Creasman DA, Nishi RA, Dumont CM, et al. Multichannel bridges and NSC synergize to enhance axon regeneration, myelination, synaptic reconnection, and recovery after SCI. NPJ Regenerative Medicine. 2024; 9: 12. https://doi.org/10.1038/s41536-024-00356-0

[9] Hornemann T, Penno A, Rütti MF, Ernst D, Kivrak-Pfiffner F, Rohrer L, et al. The SPTLC3 subunit of serine palmitoyltransferase generates short chain sphingoid bases. The Journal of Biological Chemistry. 2009; 284: 26322–26330. https://doi.org/10.1074/jbc.M109.023192

[10] Kuo A, Hla T. Regulation of cellular and systemic sphingolipid homeostasis. Nature Reviews. Molecular Cell Biology. 2024; 25: 802–821. https://doi.org/10.1038/s41580-024-00742-y

[11] He Q, Wang G, Wakade S, Dasgupta S, Dinkins M, Kong JN, et al. Primary cilia in stem cells and neural progenitors are regulated by neutral sphingomyelinase 2 and ceramide. Molecular Biology of the Cell. 2014; 25: 1715–1729. https://doi.org/10.1091/mbc.E13-12-0730

[12] Fan W, Tang S, Fan X, Fang Y, Xu X, Li L, et al. SIRT1 regulates

sphingolipid metabolism and neural differentiation of mouse embryonic stem cells through c-Myc-SMPDL3B. elife. 2021; 10: e67452. https://doi.org/10.7554/eLife.67452
[13] Murphy SM, Ernst D, Wei Y, Laurà M, Liu YT, Polke J, et al. Hereditary sensory and autonomic neuropathy type 1 (HSANI) caused by a novel mutation in SPTLC2. Neurology. 2013; 80: 2106–2111. https://doi.org/10.1212/WNL.0b013e318295d789
[14] Wang D, Sun L, Niu X, Ren L, Yang X. SphK2 promotes the progression of Helicobacter pylori-positive gastric cancer by regulating the Ras/MEK/ERK pathway. Biochemical and Biophysical Research Communications. 2025; 751: 151396. https://doi.org/10.1016/j.bbrc.2025.151396
[15] Manzo OL, Nour J, Sasset L, Marino A, Rubinelli L, Palikhe S, et al. Rewiring Endothelial Sphingolipid Metabolism to Favor S1P Over Ceramide Protects From Coronary Atherosclerosis. Circulation Research. 2024; 134: 990–1005. https://doi.org/10.1161/CIRCRESAHA.123.323826
[16] Yang W, Li Q, Pan Z. Sphingosine-1-phosphate promotes extravillous trophoblast cell invasion by activating MEK/ERK/MMP-2 signaling pathways via S1P/S1PR1 axis activation. PLoS ONE. 2014; 9: e106725. https://doi.org/10.1371/journal.pone.0106725
[17] Ullah R, Yin Q, Snell AH, Wan L. RAF-MEK-ERK pathway in cancer evolution and treatment. Seminars in Cancer Biology. 2022; 85: 123–154. https://doi.org/10.1016/j.semcancer.2021.05.010
[18] Jiang J, Hai J, Liu W, Luo Y, Chen K, Xin Y, et al. Gallic Acid Induces Neural Stem Cell Differentiation into Neurons and Proliferation through the MAPK/ERK Pathway. Journal of Agricultural and Food Chemistry. 2021; 69: 12456–12464. https://doi.org/10.1021/acs.jafc.1c04011
[19] Migita H, Kominami K, Higashida M, Maruyama R, Tuchida N, McDonald F, et al. Activation of adenosine A1 receptor-induced neural stem cell proliferation via MEK/ERK and Akt signaling pathways. Journal of Neuroscience Research. 2008; 86: 2820–2828. https://doi.org/10.1002/jnr.21742
[20] Wang QC, Lu L, Zhou HJ. Relationship between the MAPK/ERK pathway and neurocyte apoptosis after cerebral infarction in rats. European Review for Medical and Pharmacological Sciences. 2019; 23: 5374–5381. https://doi.org/10.26355/eurrev_201906_18206
[21] Jakubíková J, Sedlák J, Mithen R, Bao Y. Role of PI3K/Akt and MEK/ERK signaling pathways in sulforaphane- and erucin-induced phase II enzymes and MRP2 transcription, G2/M arrest and cell death in Caco-2 cells. Biochemical Pharmacology. 2005; 69: 1543–1552. https://doi.org/10.1016/j.bcp.2005.03.015
[22] Melchini A, Costa C, Traka M, Miceli N, Mithen R, De Pasquale R, et al. Erucin, a new promising cancer chemopreventive agent from rocket salads, shows anti-proliferative activity on human lung carcinoma A549 cells. Food and Chemical Toxicology: an International Journal Published for the British Industrial Biological Research Association. 2009; 47: 1430–1436. https://doi.org/10.1016/j.fct.2009.03.024
[23] Tarozzi A, Morroni F, Bolondi C, Sita G, Hrelia P, Djemil A, et al. Neuroprotective effects of erucin against 6-hydroxydopamine-induced oxidative damage in a dopaminergic-like neuroblastoma cell line. International Journal of Molecular Sciences. 2012; 13: 10899–10910. https://doi.org/10.3390/ijms130910899
[24] Wang T, Wu J, Dong W, Wang M, Zhong X, Zhang W, et al. The MEK inhibitor U0126 ameliorates diabetic cardiomyopathy by restricting XBP1's phosphorylation dependent SUMOylation. International Journal of Biological Sciences. 2021; 17: 2984–2999. https://doi.org/10.7150/ijbs.60459
[25] Satoh T, Nakatsuka D, Watanabe Y, Nagata I, Kikuchi H, Namura S. Neuroprotection by MAPK/ERK kinase inhibition with U0126 against oxidative stress in a mouse neuronal cell line and rat primary cultured cortical neurons. Neuroscience Letters. 2000; 288: 163–166. https://doi.org/10.1016/s0304-3940(00)01229-5
[26] Sütterlin P, Williams EJ, Chambers D, Saraf K, von Schack D, Reisenberg M, et al. The molecular basis of the cooperation between EGF, FGF and eCB receptors in the regulation of neural stem cell function. Molecular and Cellular Neurosciences. 2013; 52: 20–30. https://doi.org/10.1016/j.mcn.2012.10.006
[27] Liao W, Zheng Y, Fang W, Liao S, Xiong Y, Li Y, et al. Dual Specificity Phosphatase 6 Protects Neural Stem Cells from β-Amyloid-Induced Cytotoxicity through ERK1/2 Inactivation. Biomolecules. 2018; 8: 181. https://doi.org/10.3390/biom8040181
[28] Chen L, Xia Y, Lu J, Xie Q, Ye A, Sun W. A 50-Hz magnetic-field exposure promotes human amniotic cells proliferation via SphK-S1P-S1PR cascade mediated ERK signaling pathway. Ecotoxicology and Environmental Safety. 2020; 194: 110407. https://doi.org/10.1016/j.ecoenv.2020.110407
[29] Hait NC, Allegood J, Maceyka M, Strub GM, Harikumar KB, Singh SK, et al. Regulation of histone acetylation in the nucleus by sphingosine-1-phosphate. Science (New York, N.Y.). 2009; 325: 1254–1257. https://doi.org/10.1126/science.1176709
[30] Carpio LR, Bradley EW, Westendorf JJ. Histone deacetylase 3 suppresses Erk phosphorylation and matrix metalloproteinase (Mmp)-13 activity in chondrocytes. Connective Tissue Research. 2017; 58: 27–36. https://doi.org/10.1080/03008207.2016.1236088
[31] Caunt CJ, Keyse SM. Dual-specificity MAP kinase phosphatases (MKPs): shaping the outcome of MAP kinase signalling. The FEBS Journal. 2013; 280: 489–504. https://doi.org/10.1111/j.1742-4658.2012.08716.x
[32] Dobrowsky RT, Kamibayashi C, Mumby MC, Hannun YA. Ceramide activates heterotrimeric protein phosphatase 2A. The Journal of Biological Chemistry. 1993; 268: 15523–15530.
[33] Yu LG, Packman LC, Weldon M, Hamlett J, Rhodes JM. Protein phosphatase 2A, a negative regulator of the ERK signaling pathway, is activated by tyrosine phosphorylation of putative HLA class II-associated protein I (PHAPI)/pp32 in response to the antiproliferative lectin, jacalin. The Journal of Biological Chemistry. 2004; 279: 41377–41383. https://doi.org/10.1074/jbc.M400017200
[34] Simons K, Toomre D. Lipid rafts and signal transduction. Nature Reviews. Molecular Cell Biology. 2000; 1: 31–39. https://doi.org/10.1038/35036052
[35] Zhang Z, Wang L, Du J, Li Y, Yang H, Li C, et al. Lipid raft localization of epidermal growth factor receptor alters matrix metalloproteinase-1 expression in SiHa cells via the MAPK/ERK signaling pathway. Oncology Letters. 2016; 12: 4991–4998. https://doi.org/10.3892/ol.2016.5307
[36] Kogot-Levin A, Saada A. Ceramide and the mitochondrial respiratory chain. Biochimie. 2014; 100: 88–94. https://doi.org/10.1016/j.biochi.2013.07.027
[37] Rahimi Darehbagh R, Seyedoshohadaei SA, Ramezani R, Rezaei N. Stem cell therapies for neurological disorders: current progress, challenges, and future perspectives. European Journal of Medical Research. 2024; 29: 386. https://doi.org/10.1186/s40001-024-01987-1
[38] Boese AC, Le QSE, Pham D, Hamblin MH, Lee JP. Neural stem cell therapy for subacute and chronic ischemic stroke. Stem Cell Research & Therapy. 2018; 9: 154. https://doi.org/10.1186/s13287-018-0913-2
[39] Eckert A, Huang L, Gonzalez R, Kim HS, Hamblin MH, Lee JP. Bystander Effect Fuels Human Induced Pluripotent Stem Cell-Derived Neural Stem Cells to Quickly Attenuate Early

Stage Neurological Deficits After Stroke. Stem Cells Translational Medicine. 2015; 4: 841–851. https://doi.org/10.5966/sctm.2014-0184

[40] Gincberg G, Arien-Zakay H, Lazarovici P, Lelkes PI. Neural stem cells: therapeutic potential for neurodegenerative diseases. British Medical Bulletin. 2012; 104: 7–19. https://doi.org/10.1093/bmb/lds024

[41] De Gioia R, Biella F, Citterio G, Rizzo F, Abati E, Nizzardo M, et al. Neural Stem Cell Transplantation for Neurodegenerative Diseases. International Journal of Molecular Sciences. 2020; 21: 3103. https://doi.org/10.3390/ijms21093103